Article

Current Biology

The hierarchical radiation of phyllostomid bats as revealed by adaptive molar morphology

Graphical abstract

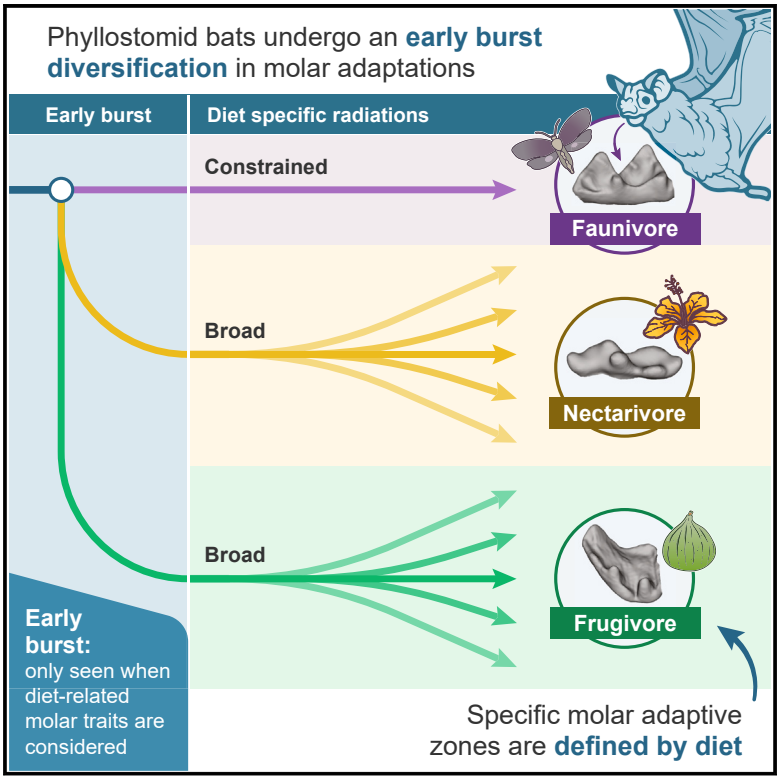

Highlights

- Phyllostomids radiated via an "early burst" only apparent in traits linked to diet
- Within-diet-group diversifications do not demonstrate early burst patterns
- The hierarchical radiation pattern seen here may be common among radiations
- Results highlight the value of using ecomorphological traits in comparative studies

Authors

David M. Grossnickle, Alexa Sadier, Edward Patterson, Nashaly N. Cortés-Viruet, Stephanie M. Jiménez-Rivera, Karen E. Sears, Sharlene E. Santana

Correspondence

david.grossnickle@oit.edu (D.M.G.), ssantana@uw.edu (S.E.S.)

In brief

To assess macroevolutionary patterns of the phyllostomid bat radiation, Grossnickle et al. use molar traits that are strongly linked to diet. The radiation is hierarchical: the initial, higher-level diversification involves a diet-driven "early burst" in morphology, and subsequent, lower-level diversifications lack an early burst pattern.

Grossnickle et al., 2024, Current Biology *34*, 1–11
March 25, 2024
https://doi.org/10.1016/j.cub.2024.02.027

CellPress

Please cite this article in press as: Grossnickle et al., The hierarchical radiation of phyllostomid bats as revealed by adaptive molar morphology, Current Biology (2024), https://doi.org/10.1016/j.cub.2024.02.027

Current Biology

CellPress

Article

The hierarchical radiation of phyllostomid bats as revealed by adaptive molar morphology

David M. Grossnickle,[1,10,*] Alexa Sadier,[2,3] Edward Patterson,[4] Nashaly N. Cortés-Viruet,[5] Stephanie M. Jiménez-Rivera,[6] Karen E. Sears,[2,7] and Sharlene E. Santana[4,8,9,*]

[1]Natural Sciences Department, Oregon Institute of Technology, Campus Drive, Klamath Falls, OR 97601, USA
[2]Department of Ecology and Evolutionary Biology, University of California, Los Angeles, Charles E. Young Drive East, Los Angeles, CA 90095, USA
[3]Institut des Sciences de l'Evolution de Montpellier, Universite de Montpellier, Place Eugene Bataillon, Montpellier 34095, France
[4]Department of Biology, University of Washington, Stevens Way NE, Seattle, WA 98195, USA
[5]Department of Animal Science, University of Puerto Rico at Mayagüez, Calle Post, Mayagüez, PR 00681, USA
[6]Caribbean Manatee Conservation Center, Inter American University of Puerto Rico, 500 Dr. John Will Harris Street, Bayamón, PR 00957, USA
[7]Department of Molecular, Cell, and Developmental Biology, University of California, Los Angeles, Charles E. Young Drive East, Los Angeles, CA 90095, USA
[8]Burke Museum of Natural History and Culture, University of Washington, Memorial Way NE, Seattle, WA 98195, USA
[9]X (formerly Twitter): @SESantanaM
[10]Lead contact
*Correspondence: david.grossnickle@oit.edu (D.M.G.), ssantana@uw.edu (S.E.S.)
https://doi.org/10.1016/j.cub.2024.02.027

SUMMARY

Adaptive radiations are bursts in biodiversity that generate new evolutionary lineages and phenotypes. However, because they typically occur over millions of years, it is unclear how their macroevolutionary dynamics vary through time and among groups of organisms. Phyllostomid bats radiated extensively for diverse diets—from insects to vertebrates, fruit, nectar, and blood—and we use their molars as a model system to examine the dynamics of adaptive radiations. Three-dimensional shape analyses of lower molars of Noctilionoidea (Phyllostomidae and close relatives) indicate that different diet groups exhibit distinct morphotypes. Comparative analyses further reveal that phyllostomids are a striking example of a hierarchical radiation; phyllostomids' initial, higher-level diversification involved an "early burst" in molar morphological disparity as lineages invaded new diet-affiliated adaptive zones, followed by subsequent lower-level diversifications within adaptive zones involving less dramatic morphological changes. We posit that strong selective pressures related to initial shifts to derived diets may have freed molars from morpho-functional constraints associated with the ancestral molar morphotype. Then, lineages with derived diets (frugivores and nectarivores) diversified within broad adaptive zones, likely reflecting finer-scale niche partitioning. Importantly, the observed early burst pattern is only evident when examining molar traits that are strongly linked to diet, highlighting the value of ecomorphological traits in comparative studies. Our results support the hypothesis that adaptive radiations are commonly hierarchical and involve different tempos and modes at different phylogenetic levels, with early bursts being more common at higher levels.

INTRODUCTION

Adaptive radiations produce novel biodiversity in response to new ecological opportunities, and they are marked by rapid increases in ecological, morphological, and taxonomic diversity.[1–6] Nonetheless, there remains uncertainty about the macroevolutionary dynamics that characterize adaptive radiations. An oft-hypothesized pattern of adaptive radiations is an "early burst" (EB) in ecomorphological change as lineages rapidly adapt to new niches, followed by a slowing of evolutionary rates as ecological opportunity diminishes.[2,7–10] Simpson's[2] seminal conceptualization of this pattern involved a rapid invasion of new adaptive zones by lineages (i.e., an "explosive phase" involving "quantum evolution"), followed by finer-scale niche partitioning within adaptive zones. However, despite the appeal and popularity of this hypothesis, the EB pattern is rarely observed in phylogenetic comparative analyses, especially those examining extant-only samples[10–16] (but see counterexamples[17–19]). The fossil record provides some support for the EB hypothesis, with clades often achieving their greatest morphological diversity early in their history.[20–24] However, it is difficult to verify if these fossil diversifications represent adaptive radiations because the available data are fragmentary and evidence linking the radiations to new ecological opportunities is often tenuous; in many cases, they could instead reflect "non-adaptive radiations."[5,25] The dearth of quantifiable EBs has led researchers to challenge the hypothesis that EBs are a common signature of adaptive radiations.[10,13]

The ability to detect EBs, however, may be hindered by multiple factors that bias the results of evolutionary model-fitting analyses, an oft-used comparative tool for inferring macroevolutionary

Please cite this article in press as: Grossnickle et al., The hierarchical radiation of phyllostomid bats as revealed by adaptive molar morphology, Current Biology (2024), https://doi.org/10.1016/j.cub.2024.02.027

patterns. For instance, the fit of an EB model[10] to morphological datasets may be weakened by a lack of fossil taxa,[11,12] small sample size, and convergent evolution among lineages of different adaptive zones.[26] The choice of traits to evaluate these patterns also heavily influences model-fitting results. Because the EB concept is associated with major ecological shifts, ecomorphological traits (e.g., tooth traits that reflect diet) are the most appropriate morphological data for testing early patterns in adaptive radiations,[4,15,27–30] but these are not always used or available. Thus, even in clades that experienced EBs, researchers may fail to observe the pattern due to methodological choices.

An expectation of Simpson's[2,7] EB model is that the macroevolutionary patterns of adaptive radiations should be hierarchical. EBs should be most common in clades that occupy multiple, distinct adaptive zones, reflecting the initial invasion of those zones, and EBs are expected to be rarer in diversifying subclades (e.g., subfamilies or genera; "local radiations" of Osborn[1]) that occupy individual adaptive zones. That is, EBs should be more common at relatively broad phylogenetic levels that include taxa of multiple adaptive zones. In support of this expectation, Slater and Friscia[29] found that ecomorphological traits associated with diet demonstrate an EB in Carnivora, but this pattern is less common in carnivoran families, which are often composed of lineages with similar ecologies. However, to the best of our knowledge, this pattern of hierarchical radiation has not been clearly demonstrated in additional taxa.

We test the hierarchical adaptive radiation hypothesis using neotropical leaf-nosed bats, family Phyllostomidae, and their close relatives (Noctilionoidea). The early diversification of phyllostomids is often categorized as an adaptive radiation; novel ecological opportunities coupled with strong selective pressures on craniodental morphology are posited to have driven the phyllostomid radiation.[31–36] Starting approximately 30 million years ago, insectivorous or omnivorous phyllostomid lineages rapidly diversified to frugivory, sanguivory, nectarivory, and vertivory[32,37–40] (Figure 1B). This dietary diversification is reflected in their extensive adaptations of the skull, jaw musculature, molars, and sensory systems.[36,37,40–51]

We apply comparative methods to lower molar shape data, which includes traits that are strongly linked to diet and thus provide ideal ecomorphologies for examining adaptive radiations.[15,28–30,51,52] We also apply the same comparative methods to body sizes, specifically basicranium widths (a proxy for size that is not strongly linked to diet in Noctilionoidea and other bats[53]) because body sizes are commonly used as ecomorphological data in macroevolutionary studies.[10,15,29] We find that phyllostomids only show evidence of an EB in molar morphology (1) at higher phylogenetic levels that include lineages that evolved into new, diet-affiliated adaptive zones and (2) for morphological traits strongly linked to diet. Thus, our results provide strong support for the hierarchical adaptive radiation hypothesis[1,2,7,29] while also highlighting the importance of phylogenetic level and trait choice in comparative studies.

RESULTS

Molar correlates of diet

In the principal component analysis (PCA) morphospace generated from the molar shape analysis (STAR Methods), noctilionoid lower molars occupy three distinct regions of PC1–2 space that correspond closely to faunivory, frugivory, and nectarivory (Figures 1C and S1). Sanguivores (vampire bats) would likely occupy a fourth region of morphospace, but they were excluded from analyses because their first lower molars are very derived, lacking homologous cusps for morphometric analyses (Figure S3).

We describe PC1–2 as "molar correlates of diet" because they are the only PCs (of PC1–30) from the molar shape analysis that demonstrate statistical differences among diet groups (via phylogenetic (p)ANOVAs; $p < 0.0001$ for PC1 and PC2; Table S1), and they are the only PCs to account for more variance than expected by chance via a "broken-stick" model[54] (Figure S4). Functional considerations also support the link between PC1–2 and diet (summarized in Table 1). PC1 (39% of variance) largely captures cusp heights relative to overall tooth height, with faunivores (positive PC1 scores) having relatively tall cusps (Figure 1C). Cusp height largely influences the molar relief index (the ratio of 3D surface area to 2D surface area), which exhibits a strong association with mammalian diet and feeding performance.[51,52,55] PC2 (23% of variance) reflects differences in molar width, with frugivores having relatively wide molars (positive PC2 scores), likely reflecting greater occlusal areas for crushing/grinding fruit pulp and seeds.[51]

Morphological disparity patterns

When using only molar correlates of diet (PC1–2), there is a distinct decrease in average subclade disparity (blue arrow in Figure 2A) at the node that we refer to as "Phyllostomidae*" (red star in Figures 1B and 2A), which is where early diverging lineages Lonchorhinini, Micronycterini, and Macrotinae split from the rest of Phyllostomidae and most dietary diversity begins to arise. Morphological disparity index (MDI) results indicate that the average subclade disparity is lower than expected by chance for the major focal nodes in this study (Noctilionoidea, Phyllostomidae, and Phyllostomidae*; Table 2), consistent with an EB pattern.[8,56] However, the distinct decrease in subclade disparity at the Phyllostomidae* node is less pronounced when including molar shape data unrelated to diet (PC1–30; Figure 2B), and subclades instead show elevated disparity until the present (blue arrow in Figure 2B). It is worth noting that Harmon et al.[8] recommended excluding the most recent third of the disparity-through-time plot because biases could artificially increase average subclade disparity, and thus the elevated disparity observed here for all molar data (PC1–30; Figure 2B) should be considered with caution.

Node height tests are not statistically significant when using the full noctilionoid sample or any of the individual diet groups (Table S2). However, the tests are statistically significant for Phyllostomidae and Phyllostomidae* for both PC1 and PC2 (Table S2), which is consistent with an EB.

Among diet groups, frugivore molars have the greatest morphological disparity (variance of tip data), stationary variance (STAR Methods), and evolutionary rates (σ^2 from the BMM3 model). Conversely, faunivore molars exhibit low disparity levels and slow rates (Tables 2 and S2). Basicranium width (proxy for body size), which is not statistically different among diet groups (Table S1), exhibits a very different pattern than that of molars, with faunivores having the greatest disparity, stationary variance, and evolutionary rates (Tables 2 and S2).

Please cite this article in press as: Grossnickle et al., The hierarchical radiation of phyllostomid bats as revealed by adaptive molar morphology, Current Biology (2024), https://doi.org/10.1016/j.cub.2024.02.027

CellPress

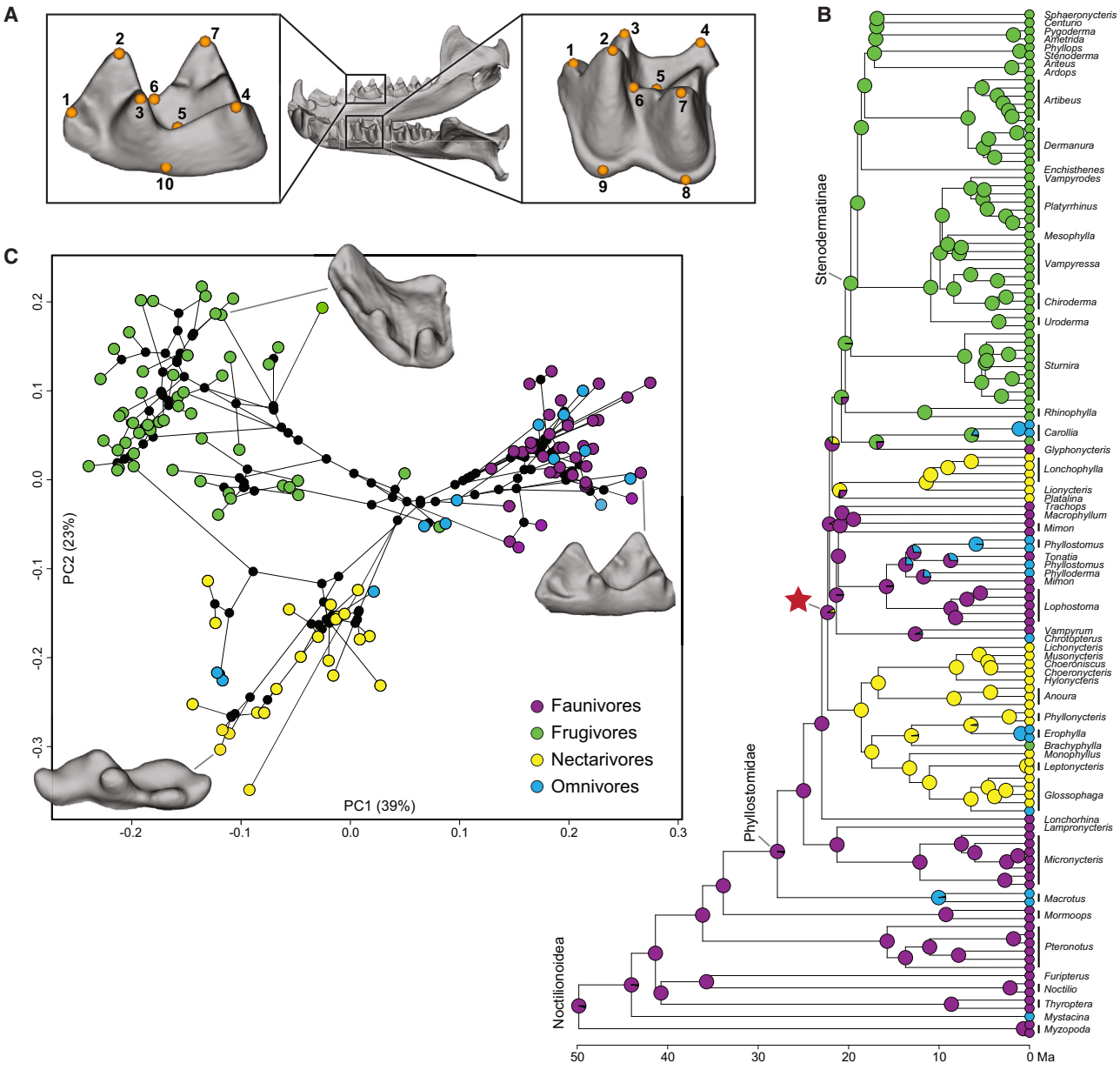

Figure 1. Molars, phylogeny, and phylomorphospace of noctilionoid bats

(A and B) The molar landmarking scheme (A) and phylogeny (B) used in this study, with diets at ancestral nodes being summaries from 100 SIMMAP reconstructions. Landmark coordinates are provided in Data S1C, and Figure S1 illustrates an alternative landmark scheme.

(C) The PC1–2 phylomorphospace plot highlights the distinct ecomorphotypes associated with faunivory, frugivory, and nectarivory, with ancestral diets at nodes based on maximum likelihood estimates. See Figure S2 for a PCA plot with species labeled.

The specimen images are *Lophostoma silvicolum* (A; AMNH 64029), *Sphaeronycteris toxophyllum* (frugivore; AMNH 262637), *Lampronycteris brachyotis* (faunivore; AMNH 175639), and *Musonycteris harrisoni* (nectarivore; UMMZ 110524). The red star in (B) marks the node at which the first non-faunivore/omnivore lineages arise (Phyllostomidae*; see text).

Adaptive zone mapping

We performed two sets of model-fitting analyses to the molar shape data: (1) "full-sample analyses" that examine the overall adaptive landscape of noctilionoids and include a suite of models (single-regime, shift, and multiple-regime) and (2) "subgroup analyses" that examine macroevolutionary patterns within diet groups and less inclusive clades (STAR Methods; Tables 3 and S3). For analyses using molar data (either PC1–2 or PC1–6, 85% of variance), the overwhelmingly best-fitting model is BMM3, a multiple-regime Brownian motion (BM) model that allows evolutionary rates to vary between regimes (i.e., diet groups) and uses a three-diet classification scheme (faunivory, frugivory, and nectarivory). Although the second-best-fitting model is BMM4 (with omnivores as a regime), the considerably better fit of the BMM3 model suggests that there is not a distinct omnivore ecomorphotype, which is consistent with studies of

Please cite this article in press as: Grossnickle et al., The hierarchical radiation of phyllostomid bats as revealed by adaptive molar morphology, Current Biology (2024), https://doi.org/10.1016/j.cub.2024.02.027

Table 1. Summary of the morphological and functional traits captured by the molar correlates of diet (PC1–2)

	Morphological traits	Functional traits	Diet differentiation
PC1	cusp heights; species with relatively taller cusps have positive PC1 scores	degree of puncturing or slicing capabilities, with faunivores best adapted for these functions	faunivores separate from herbivores (frugivores, nectarivores)
PC2	molar width; species with relatively wider molars have positive PC2 scores	degree of crushing or grinding capabilities, with frugivores best adapted for these functions	frugivores + faunivores separate from nectarivores

bat upper molars[44] and mammalian jaws.[15] For the analyses of basicranium width (body size), OUBMi is the best-fitting model. OUBMi is the "release and radiate" model of Slater,[57] which allows for a rate change with the shift between modes.

The presence of three diet-affiliated adaptive zones is independently supported by the supplemental *phyloEM*[59] model-fitting analyses, which do not include a priori regime (diet) assignments. The PC1–2 analysis identified three regime shifts; two at the bases of the major nectarivore clades and one at the base of Stenodermatinae, which accounts for most frugivores in our sample (Figure S5). The lack of a regime shift in faunivore clades is consistent with our conclusion that they exhibit the ancestral molar morphology. The PC1–6 analysis identified many more regime shifts (13 shifts with >400 equivalent shift solutions), suggesting less correlation with dietary changes compared with the shifts in the PC1–2 analysis.

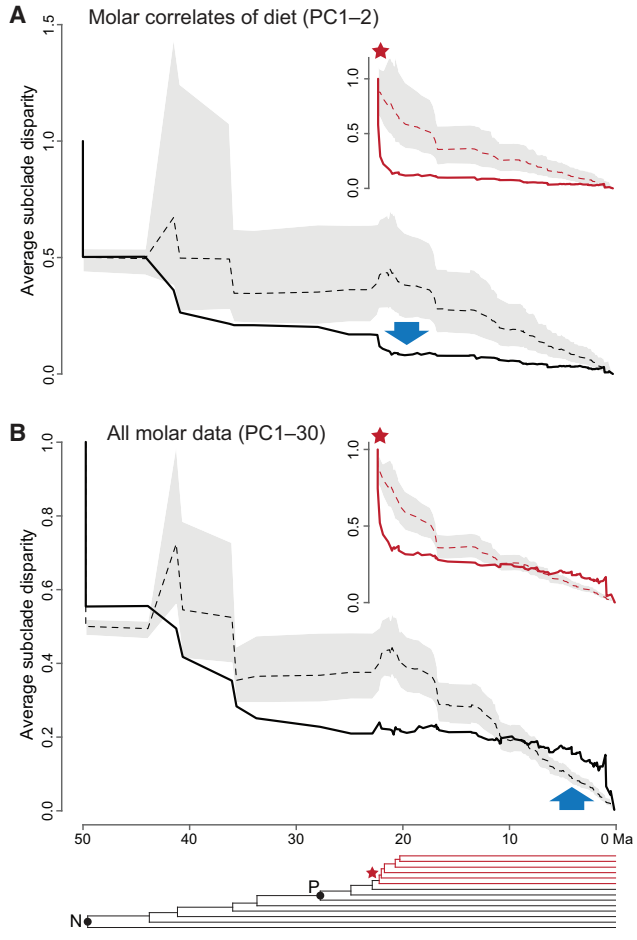

Figure 2. Disparity-through-time patterns for noctilionoid molars suggest a "burst" at the Phyllostomidae* node (red star)

Subclade disparity-through-time using PC1–2 scores (diet correlates; A) and all PCs (B) from the geometric morphometrics analysis of noctilionoid molar shape. Solid lines are empirical data, and dashed lines are simulated data with confidence intervals. Blue arrows highlight the major differences between the results of the two analyses. Analyses were repeated using only taxa defined by the node denoted by the red star (Phyllostomidae*; red lines), which includes most phyllostomids except for early branching faunivores (Figure 1B). The phylogeny is a simplified version of the phylogeny in Figure 1B, with Noctilionoidea (N) and Phyllostomidae (P) labeled.

For the subgroup analyses, we fitted single-regime models (single-regime Brownian motion model [BM1], single-regime Ornstein-Uhlenbeck model [OU1], EB) to Noctilionoidea, Phyllostomidae, and Phyllostomidae*, in addition to groups that only include species of one diet (faunivores, frugivores, and nectarivores). An EB model is the best-fitting model in analyses that (1) include multiple diet groups and (2) use molar correlates of diet (PC1–2; Figures 3A–3C; Table S3). For the EB model fit to Phyllostomidae* PC1–2, the rate decay half-life is 6.8 million years (Table S2), which indicates that 3.5 rate half-lives have elapsed during the clade's history and supports our interpretation of an EB pattern.[26] Further, when including a greater number of molar shape axes (PC1–6), the EB models perform best for the Phyllostomidae analysis (with BM statistically similar, ΔAICc [Akaike information criterion] < 2) and Phyllostomidae* analysis. The EB model performs poorly in all other analyses, except for frugivore molar correlates of diet, in which it is the second-best-performing model (ΔAICc < 2; Figure 3E; Table S3). Also, when using an alternative landmarking scheme for frugivores (STAR Methods; Figure S1), the EB model is the best-performing model, although BM1 is statistically similar with ΔAICc < 1 (Table S6). For basicranium width, the EB model always collapses to a BM model (i.e., the rate decay parameter is zero), and OU1 is the best-fitting model for all three-diet groups (Figure 3).

The strong fits of EB models to PC1–2 (Figure 3; Table S3) could be due in part to bias toward an EB model when fitting models to PCs.[60] However, multiple lines of evidence, including the independent identification of an EB by multiple analyses in this study (Tables 2 and S2), suggest our results are robust to this potential bias. Further, our model-fitting analyses are multivariate and incorporate correlation between PCs, which is less problematic than fitting univariate models to individual PCs.[58,60] Thus, we believe that our central conclusions are robust to potential biases associated with fitting models to PCs.

DISCUSSION

The macroevolutionary patterns of phyllostomid molars are consistent with predictions of the hierarchical adaptive radiation hypothesis.[1,2,7,29] The phyllostomid radiation involved (1) a dramatic higher-level radiation of lineages into novel, diet-affiliated adaptive zones and (2) lower-level radiations of lineages within

Please cite this article in press as: Grossnickle et al., The hierarchical radiation of phyllostomid bats as revealed by adaptive molar morphology, Current Biology (2024), https://doi.org/10.1016/j.cub.2024.02.027

CellPress

Table 2. Morphological disparities and evolutionary rates of molar shape for focal clades and diet groups

	Disparity			MDI			Rate		
Sample	PC1–2	All PCs	Body size	PC1–2	All PCs	Body size	PC1	PC2	Body size
Noctilionoidea	0.042	0.067	0.051	−0.170***	−0.069***	0.997	–	–	–
Phyllostomidae	0.042	0.067	0.038	−0.237***	−0.115***	0.002	–	–	–
Phyllostomidae*	0.039	0.066	0.038	−0.240***	−0.073**	0.066	–	–	–
Faunivores	0.004	0.022	0.091	0.033	0.126	0.648	0.00007	0.00008	0.01090
Frugivores	0.012	0.045	0.025	−0.032	0.103	0.194	0.00025	0.00031	0.00240
Nectarivores	0.007	0.030	0.011	−0.064	0.163	0.307	0.00015	0.00025	0.00116

Morphological disparity is calculated as the sum of variances. For the morphological disparity index (MDI), statistical significance is as follows: *$p < 0.05$, **$p < 0.01$, and ***$p < 0.001$. Evolutionary rates are the fitted σ^2 parameters from the BMM3 model, which is the best-fitting model for the full-sample analyses. BMM3 allows rates to vary among diet-defined selective regimes. See Tables S2 and S4 for related results.

adaptive zones. The tempos and modes of evolution of these two levels of radiation vary considerably, with the higher-level radiation involving relatively faster, more extreme morphological changes consistent with an EB pattern. We conceptualize our interpretation of this hierarchical radiation in Figure 4, and the following subsections discuss evidence for these patterns.

Table 3. Evolutionary model-fitting analyses that examine the overall adaptive landscape of Noctilionoidea (full-sample analyses)

	Molar shape				Body size	
	PC1–2 (diet correlates)		PC1–6		Basicranium widths	
Model	ΔAICc	Weight	ΔAICc	Weight	ΔAICc	Weight
Single regime						
BM1	166.560	<0.001	315.248	<0.001	88.373	<0.001
OU1	172.918	<0.001	305.181	<0.001	54.987	<0.001
EB	144.771	<0.001	321.175	<0.001	90.475	<0.001
Shift						
OUBMi[a]	128.534	<0.001	226.683	<0.001	0.000[a]	>0.999[a]
OUBM	134.891	<0.001	226.961	<0.001	80.275	<0.001
OUEB	103.638	<0.001	222.273	<0.001	27.092	<0.001
BMEB	164.401	<0.001	305.453	<0.001	51.887	<0.001
BMBM	134.926	<0.001	237.805	<0.001	40.406	<0.001
Multiple regime						
BMM4	19.899	<0.001	48.238	<0.001	53.520	<0.001
BM1m4	55.453	<0.001	212.451	<0.001	93.566	<0.001
OUM4	55.255	<0.001	185.496	<0.001	51.104	<0.001
BMM3[a]	0.000[a]	>0.999[a]	0.000[a]	>0.999[a]	49.161	<0.001
BM1m3	35.147	<0.001	183.489	<0.001	91.407	<0.001
OUM3	49.784	<0.001	181.009	<0.001	57.071	<0.001

The shift models test for changes in mode of evolution at Phyllostomidae*. The OUBMi model, which is the best-fitting model to basicranium widths, allows different rates between the two modes.[57] The numbers at the end of multiple-regime model names ("3" or "4") represent the number of diet-defined selective regimes, and BM1m models differ from BMM models by modeling a single rate among regimes. For multiple-regime models, the results are median values from fitted models to 25 SIMMAP trees. See the STAR Methods for complete model descriptions, and see Table S5 for related results. ΔAICc values are the small-sample-size corrected Akaike information criterion values, and the "weights" are Akaike weights. Models were fitted to data using functions in the *mvMORPH* R package.[58] See Table S5 for related results.
[a]Best-fitting models

Higher-level radiation—EB

The adaptive landscape of Noctilionoidea molars likely includes at least three broad, diet-affiliated adaptive zones (Figure 4), as evidenced by the significant differences in molar shapes among diet groups (Figure 1C; Table S1), strong fit of the BMM3 model to molar shape data (Table 3), and identification of regime shifts by the *phyloEM* analysis that correspond to diet shifts (Figure S5). The initial phyllostomid radiation also likely included the evolution of sanguivores,[34,38,61] which we excluded from analyses due to their extremely derived, reduced molars (Figure S3). Thus, a sanguivore adaptive zone is also likely present and it may be in an outlying position beyond those of faunivores (due to relatively tall cusps compared with overall molar size) and/or nectarivores (due to relatively thin molars) in molar morphospace. Our results are consistent with inferences of the phyllostomid adaptive landscape based on jaw shape,[14,42,62] although Monteiro and Nogueira[42] found evidence that two faunivore subgroups (vertivores and insectivores) occupy separate adaptive zones. The small number of phyllostomid vertivore species prohibited us from rigorously testing for a distinct vertivore adaptive zones, but vertivore species do not appear to separate from insectivores in our molar morphospace (Figures 1C and S2) and the *phyloEM* analysis of PC1–2 did not identify a regime shift within faunivores (Figure S5).

The invasion of frugivore and nectarivore adaptive zones likely occurred during a diet-affiliated, Simpsonian EB at or near the Phyllostomidae* node (Figures 2 and 3; Tables 2 and S3). EB models outperformed other single-regime models (BM1 and OU1) in clades that include multiple diet groups (Figures 3A–3C), and an EB pattern is supported by the disparity-through-time plots (Figure 2), statistically significant MDI results (Table 2), and relatively short EB model rate decay half-lives (Table S2). Although we find evidence of an EB at all tested phylogenetic levels, the strongest evidence is at the Phyllostomidae* node (Figures 2 and 3; Tables 2 and S2), which is where most dietary diversity begins to arise in Phyllostomidae (Figure 1B).

Multiple-regime models outperform EB models in the "full-sample" analyses (Table 3), consistent with previous studies in which multiple-regime models better explain patterns of radiating clades—in agreement with a Simpsonian EB.[14,63] A

Please cite this article in press as: Grossnickle et al., The hierarchical radiation of phyllostomid bats as revealed by adaptive molar morphology, Current Biology (2024), https://doi.org/10.1016/j.cub.2024.02.027

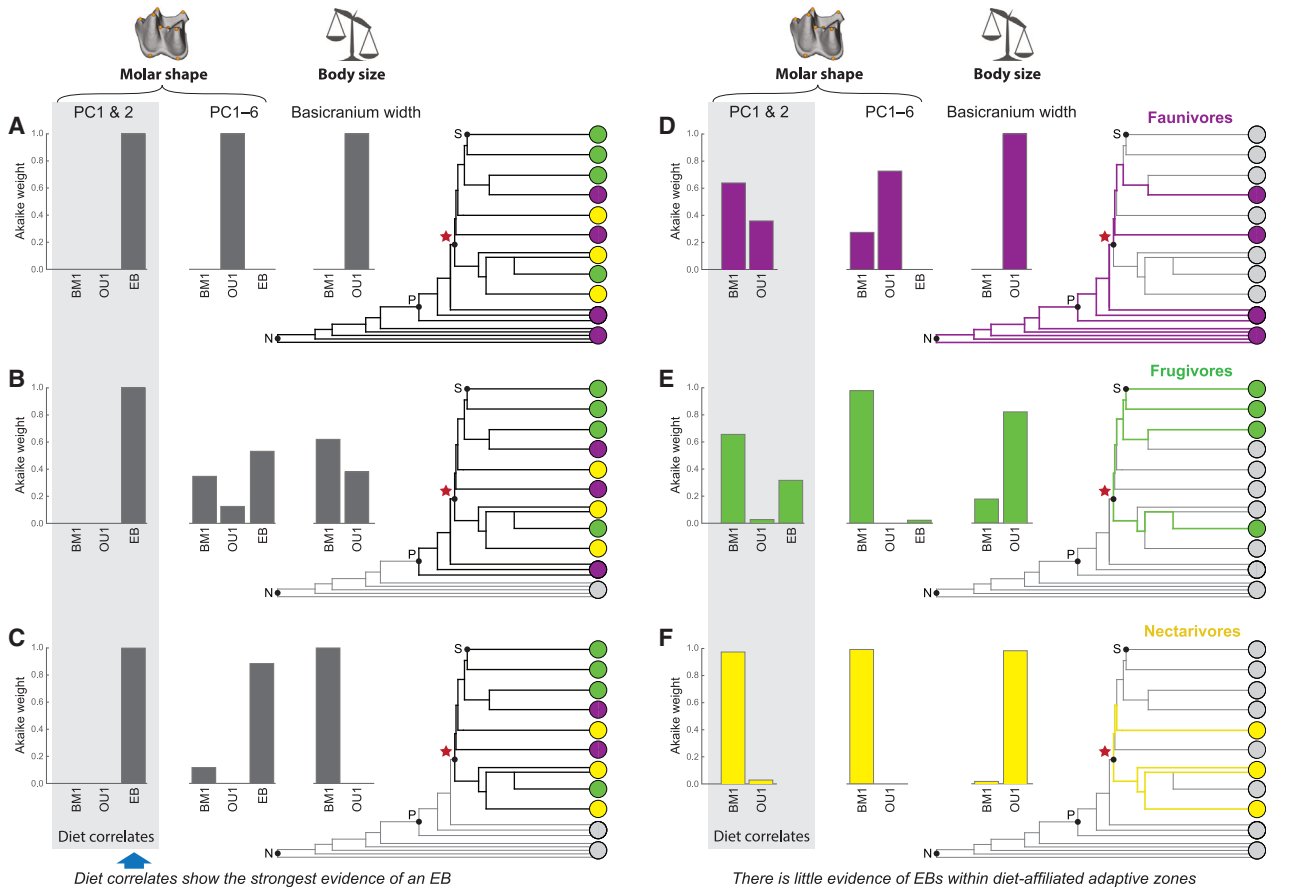

Figure 3. Evolutionary model-fitting analyses suggest an early burst but only when using molar correlates of diet

Model-fitting analyses testing the influence of node choice (A–C) and examining patterns within diet-affiliated adaptive zones (D–F). These subgroup analyses only include single-regime models. Prior to each analysis, we pruned the phylogeny to the focal lineages; the excluded lineages are colored gray. We used the three-diet scheme (excluding omnivory as a separate group) because multiple-regime models using the three-diet scheme outperformed the four-diet-scheme models (Table 2). Each analysis was repeated using three morphological datasets:molar shape PC1–2, molar shape PC1–6, and log-transformed basicranium width. EB model results are excluded when the decay rate parameter is zero because the model collapses to a BM model. The phylogeny is a simplified version of that in Figure 1B; sister taxa with shared diets are condensed into single lineages, and some lineages are illustrated as being paraphyletic for simplicity. See Tables S3 and S6 for related results. BM1, single-regime Brownian motion model; EB, early burst model; N, Noctilionoidea; OU1, single-regime Ornstein-Uhlenbeck model; P, Phyllostomidae; "red star," Phyllostomidae*; S, Stenodermatinae.

potential reason for this result is that morphological convergence resulting from shifts between adaptive zones can weaken support for EB models[26] in favor of multiple-regime models.[63] Multiple phyllostomid lineages independently evolved both nectarivory and frugivory[31] (Figure 1B), resulting in morphological convergence (Figure 1C). Nonetheless, the EB model is best-fitting among single-regime models and the OUEB model (with a shift to an EB mode of evolution at Phyllostomidae*) is the best-fitting "shift" model (Figures 3A–3C; Table 3), indicating that among the simpler classes of models there is strong support for an EB.

The scarcity of species in morphospace regions between diet groups suggests the presence of adaptive valleys (Figures 1C and 4). This raises the question as to how phyllostomid lineages crossed these valleys. Previous research suggests that early phyllostomids were omnivorous[37,38,40,64] and, as an ecological strategy, omnivory may have helped lineages transverse adaptive valleys. Omnivores and insectivores often have similar molar morphologies,[44] with omnivores primarily occupying the faunivore region of morphospace (Figure 1C). Nonetheless, as omnivorous lineages evolve a more plant-dominated diet, molars may shift to a functional trade-off morphology that is intermediate to those of faunivores and herbivores.[65] Freeman[33] suggested that this type of intermediate morphology is exhibited by *Carollia* species, which are primarily plant-dominated omnivores and centrally positioned in morphospace (Figure S2). As ancestral omnivores fully shifted to frugivory and nectarivory, strong selective pressures likely drove major changes in craniodental morphology.[31–35] This is supported by the major axes of variation (PC1–2) being strongly liked to diet (Figure 1C; Table S1) and accounting for more variance than expected by chance (Figure S4). Crossing the adaptive valleys may have also been facilitated by developmental biases, which can constrain or facilitate morphological evolution.[66–68] For instance, the novel acquisition of cusps during mammal evolution has been linked to signaling and growth factor variation, allowing tooth morphologies to

Please cite this article in press as: Grossnickle et al., The hierarchical radiation of phyllostomid bats as revealed by adaptive molar morphology, Current Biology (2024), https://doi.org/10.1016/j.cub.2024.02.027

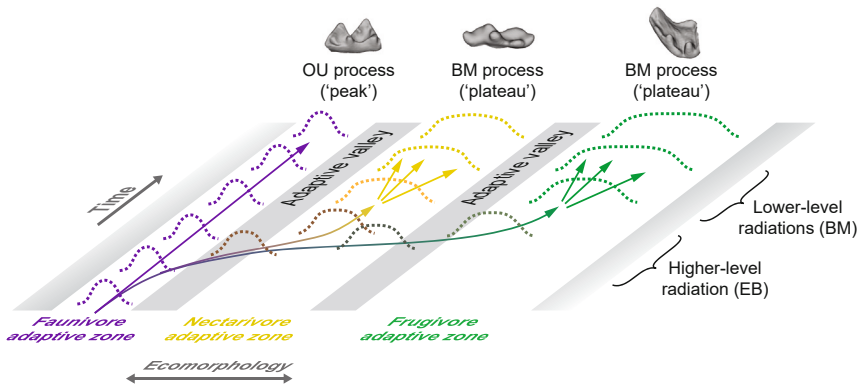

Figure 4. Conceptualization of the hierarchical radiation of phyllostomid bats

Inspired by illustrations of quantum evolution and adaptive zones by Simpson.[2] The higher-level radiation of phyllostomids exhibits an early burst (EB) pattern (Simpson's explosive phase), but within-zone radiations are best described by Brownian motion (BM) or Ornstein-Uhlenbeck (OU) processes (Simpson's "normal phase").

escape constraints and cross over to new adaptive zones.[68] Similarly, bats seem to have overcome ancestral developmental constraints to evolve a large range of derived dental morphologies.[69]

The EB in molar morphology appears to be driven by major diet-related adaptations because the EB pattern dissipates when using morphological traits that are not correlated with diet. Body size, which is not correlated with the diet categories examined here, and non-diet-correlated molar traits show reduced evidence of an EB (Figures 2 and 3; Tables 2 and S3). This highlights that results of comparative analyses may be especially sensitive to researchers' choice of input data. It also demonstrates the importance of using ecomorphological (versus morphological) traits in comparative analyses—we would have missed the strong EB pattern if we had not performed analyses using only molar correlates of diet (PC1–2). Therefore, we advocate the use of morphological traits that are strongly linked to ecology within focal clades, and we echo recent arguments against relying solely on body size data in macroevolutionary comparative studies.[15,29]

Lower-level radiations—Unique tempos and modes within adaptive zones

In contrast to the higher-level EB radiation, molar diversifications within diet-affiliated adaptive zones are best described by a BM process (frugivores and nectarivores) or an OU process (faunivores; Figure 3; Tables 3 and S3). The EB model is the second-best-fitting model in the frugivore analysis (Figure 3E; see Dumont et al.[33]), but its rate decay half-life is relatively long (18.5 million years when using PC1–6; Table S2) with only one half-life having elapsed, suggesting a weak EB pattern.[26] In addition, frugivores' MDI (Table 2) and node height test results (Table S2) are both not significant and therefore inconsistent with a strong EB. Sanguivores, which are not analyzed here, have reduced molars that appear morphologically similar among species, and thus it is unlikely that they experienced an EB.

The adaptive landscape topography varies among diet groups and may reflect varying functions of molar ecomorphotypes. Faunivore molars, which represent the ancestral ecomorphotype (Figure 1), are best fitted by an OU model, suggesting an adaptive peak with strong selective pressures maintaining the ancestral, dilambdodont tribosphenic molar morphology that has remained relatively unchanged during chiropteran history.[37,70] This is supported by evidence of faunivores occupying a relatively small region of morphospace and exhibiting slow evolutionary rates (Figure 1C; Tables 2 and S2). The low level of disparity in this ecomorphotype is possibly due to strong selective pressures related to maintaining a functional tribosphenic molar, which requires precise occlusion of multiple shearing crests,[71,72] and small morphological changes could disrupt proper function to a greater degree than similar changes in frugivores and nectarivores. Further, the ancestral tribosphenic molar morphology likely evolved early in mammalian history (ca. 160 Ma[73]), possibly resulting in well-established developmental constraints. Although faunivores did not morphologically diversify, they may still have experienced ecological diversification via one-to-many mapping of form to function (i.e., a single molar morphotype is well suited for multiple diets). For instance, extant noctilionoid faunivores include taxa with specialized diets such as piscivory and vertivory (Data S1A).

In contrast to faunivores, the strong fits of BM models in frugivore-only and nectarivore-only analyses suggest that these diet groups occupy relatively broad adaptive zones, which could be conceptualized as adaptive "plateaus" (Figure 4). The interpretation of broad adaptive plateaus is supported by high disparity levels and fast evolutionary rates compared with those of faunivores (Table 2). After early lineages of these diet groups crossed adaptive valleys and reached adaptive plateaus, we posit that they continued to diversify morphologically rather than be constrained to a specific adaptive peak (Figure 1C). This continued diversification is reflected in disparity-through-time results that show elevated subclade disparity until the present when using all molar data (blue arrow in Figure 2B). Therefore, whereas molar correlates of diet show a diversification near Phyllostomidae*, additional molar traits continued to diversify within adaptive zones, maintaining the prolonged elevated disparity. The traits that continue to diversify may be associated with finer-scale resource partitioning as lineages saturated adaptive zones.

The relatively high level of molar disparity in frugivores (Table 2), in addition to EB being their second-best-fitting model (Figure 3E), could reflect adaptations for consuming a diversity of fruit types. Phyllostomid frugivores may specialize in soft, small-seeded fruits[74]; hard, large-seeded fruits[75]; or seed predation,[76] or may have generalized fruit diets. Some molar features (e.g., rim on the labial side of the molar, large trigonid basin[77]) are posited to relate to specialization on these narrower diets. In contrast, nectarivores use their tongues for ingesting nectar and rely less on molars for feeding (although they may still masticate some insects and fruit pulp[78]). Thus, there may have been a relaxation of selective pressures on nectarivore molar shape,

allowing diversification via stochastic processes such as drift, which is supported by the especially strong fit of a BM model (Figure 3F). Further, the evolutionary lengthening and narrowing of the nectarivore jaw[49] (Figure S3) may have helped drive the evolution of their relatively long and narrow molars.[63]

Beyond the evidence highlighted here, a hierarchical pattern during adaptive radiations is supported by the hypothesis that radiations occur in stages, with each stage associated with a different resource axis.[79] However, this idea is based primarily on radiations at relatively smaller phylogenetic levels without major shifts between adaptive zones.[9,27,30,79] Thus, our study provides novel insight on evolutionary processes at higher scales, with a focus on a critical resource axis (i.e., diet) that likely drove the EB pattern.

Conclusions

In their discussion of macroevolutionary patterns, Slater and Friscia[29] concluded, "The critical question facing comparative evolutionary biologists is, we argue, not whether EB adaptive radiation occurs but, rather, at what phylogenetic levels and in which niche traits it is most common." Here, we answer that question for phyllostomids, finding that they experienced a family-level EB radiation that was associated with dietary diversification. Importantly, this EB pattern is most apparent when examining molar traits that are strongly linked to diet. Further, the strength of the EB pattern is influenced by the choice of clade used in analyses, with Phyllostomidae and Phyllostomidae* showing stronger signals than Noctilionoidea (Figures 2 and 3; Tables 2 and S2). In analyses using traits not correlated with diet (body size and molar traits), the evidence for an EB is greatly reduced, highlighting the influence of trait choice and the importance of using ecomorphological traits in comparative analyses.

After the phyllostomid EB, subsequent within-adaptive-zone diversifications among derived dietary groups (frugivores and nectarivores) resulted in the groups occupying broad adaptive zones (or adaptive plateaus). The unique tempos and modes of evolution of different diet groups are likely linked to varying levels of selective pressures and functional demands on different molar ecomorphotypes. Thus, we interpret the phyllostomid radiation to be hierarchical, with an EB only present at a higher phylogenetic levels that captures the invasion of new adaptive zones, followed by finer-scale niche partitioning as lineages diversified within newly invaded, broad adaptive zones (Figure 4). This lends strong support to the hierarchical adaptive radiation hypothesis,[1,2,29] and suggests that a hierarchical pattern may be common, yet underappreciated, among adaptive radiations.

STAR★METHODS

Detailed methods are provided in the online version of this paper and include the following:

- KEY RESOURCES TABLE
- RESOURCE AVAILABILITY
  - Lead contact
  - Materials availability
  - Data and code availability
- EXPERIMENTAL MODEL AND STUDY PARTICIPANT DETAILS
- METHOD DETAILS
- QUANTIFICATION AND STATISTICAL ANALYSIS
  - Geometric morphometrics and analyses of PCs
  - Evolutionary model-fitting analyses
  - Morphological disparity

SUPPLEMENTAL INFORMATION

Supplemental information can be found online at https://doi.org/10.1016/j.cub.2024.02.027.

ACKNOWLEDGMENTS

Nancy Simmons and Marisa Surovy facilitated access to specimens in the mammal collection at the AMNH, and Jeff Bradley assisted with specimens at the UWBM. We thank Jeff J. Shi, Cody W. Thompson, and Daniel L. Rabosky for providing access to specimen scans through the MorphoSource repository (www.morphosource.org), with funding for their research assisted by the National Science Foundation (NSF) DEB 1501307. We also thank the managers and funders of MorphoSource. Funding for this study was provided by the NSF (IOS 2017738 to S.E.S. and IOS 2017803 to K.E.S.). Jennifer Gardner, Adam P. Summers, David Villalobos-Chaves, and Kathryn E. Stanchak provided assistance with micro-computed tomography (micro-CT) scanning of specimens. For feedback on methods and earlier drafts of the manuscript, we thank two anonymous reviewers, Lucas N. Weaver, Graham J. Slater, P. David Polly, A. Murat Maga, Sara Rolfe, William H. Brightly, members of the Santana lab, and the University of Washington Paleo Lunch group. Nuria Melisa Morales Garcia and Emily Green assisted with the graphical abstract.

AUTHOR CONTRIBUTIONS

Conceptualization, D.M.G. and S.E.S.; methodology, D.M.G.; investigation, D.M.G., E.P., N.N.C.-V., and S.M.J.-R.; writing, D.M.G., A.S., E.P., N.N.C.-V., S.M.J.-R., and K.E.S.; resources, S.E.S.; funding acquisition, A.S., K.E.S., and S.E.S.

DECLARATION OF INTERESTS

The authors declare no competing interests.

Received: September 4, 2023
Revised: December 11, 2023
Accepted: February 13, 2024
Published: March 5, 2024

REFERENCES

1. Osborn, H.F. (1902). The law of adaptive radiation. Am. Nat. *36*, 353–363.
2. Simpson, G.G. (1944). Tempo and Mode in Evolution (Columbia University Press).
3. Erwin, D.H. (1992). A preliminary classification of evolutionary radiations. Hist. Biol. *6*, 133–147.
4. Schluter, D. (2000). The Ecology of Adaptive Radiation (Oxford University Press).
5. Givnish, T.J. (2015). Adaptive radiation versus 'radiation' and 'explosive diversification': why conceptual distinctions are fundamental to understanding evolution. New Phytol. *207*, 297–303.
6. Stroud, J.T., and Losos, J.B. (2016). Ecological opportunity and adaptive radiation. Annu. Rev. Ecol. Evol. Syst. *47*, 507–532.
7. Simpson, G.G. (1953). The Major Features of Evolution (Columbia University Press).
8. Harmon, L.J., Schulte, J.A., Larson, A., and Losos, J.B. (2003). Tempo and mode of evolutionary radiation in iguanian lizards. Science *301*, 961–964.

9. Gavrilets, S., and Losos, J.B. (2009). Adaptive radiation: contrasting theory with data. Science *323*, 732–737.
10. Harmon, L.J., Losos, J.B., Jonathan Davies, T., Gillespie, R.G., Gittleman, J.L., Bryan Jennings, W., Kozak, K.H., McPeek, M.A., Moreno-Roark, F., Near, T.J., et al. (2010). Early bursts of body size and shape evolution are rare in comparative data. Evolution *64*, 2385–2396.
11. Slater, G.J., Harmon, L.J., and Alfaro, M.E. (2012). Integrating fossils with molecular phylogenies improves inference of trait evolution. Evolution *66*, 3931–3944.
12. Mitchell, J.S. (2015). Extant-only comparative methods fail to recover the disparity preserved in the bird fossil record. Evolution *69*, 2414–2424.
13. Pincheira-Donoso, D., Harvey, L.P., L.P., and Ruta, M. (2015). What defines an adaptive radiation? Macroevolutionary diversification dynamics of an exceptionally species-rich continental lizard radiation. BMC Evol. Biol. *15*, 1–13.
14. Arbour, J.H., Curtis, A.A., and Santana, S.E. (2019). Signatures of echolocation and dietary ecology in the adaptive evolution of skull shape in bats. Nat. Commun. *10*, 2036.
15. Grossnickle, D.M. (2020). Feeding ecology has a stronger evolutionary influence on functional morphology than on body mass in mammals. Evolution *74*, 610–628.
16. Weaver, L.N., and Grossnickle, D.M. (2020). Functional diversity of small-mammal postcrania is linked to both substrate preference and body size. Curr. Zool. *66*, 539–553.
17. Arbour, J.H., and López-Fernández, H. (2013). Ecological variation in South American geophagine cichlids arose during an early burst of adaptive morphological and functional evolution. Proc. Biol. Sci. *280*, 20130849.
18. Price, S.L., Etienne, R.S., and Powell, S. (2016). Tightly congruent bursts of lineage and phenotypic diversification identified in a continental ant radiation. Evolution *70*, 903–912.
19. Stanchak, K.E., Arbour, J.H., and Santana, S.E. (2019). Anatomical diversification of a skeletal novelty in bat feet. Evolution *73*, 1591–1603.
20. Foote, M. (1994). Morphological disparity in Ordovician-Devonian crinoids and the early saturation of morphological space. Paleobiology *20*, 320–344.
21. Erwin, D.H. (2007). Disparity: morphological pattern and developmental context. Palaeontology *50*, 57–73.
22. Hughes, M., Gerber, S., and Wills, M.A. (2013). Clades reach highest morphological disparity early in their evolution. Proc. Natl. Acad. Sci. USA *110*, 13875–13879.
23. Grossnickle, D.M., Smith, S.M., and Wilson, G.P. (2019). Untangling the multiple ecological radiations of early mammals. Trends Ecol. Evol. *34*, 936–949.
24. Zhang, X., and Shu, D. (2021). Current understanding on the Cambrian Explosion: questions and answers. PalZ *95*, 641–660.
25. Erwin, D.H. (2015). Novelty and innovation in the history of life. Curr. Biol. *25*, R930–R940.
26. Slater, G.J., and Pennell, M.W. (2014). Robust regression and posterior predictive simulation increase power to detect early bursts of trait evolution. Syst. Biol. *63*, 293–308.
27. Colombo, M., Damerau, M., Hanel, R., Salzburger, W., and Matschiner, M. (2015). Diversity and disparity through time in the adaptive radiation of Antarctic notothenioid fishes. J. Evol. Biol. *28*, 376–394.
28. Feilich, K.L., and López-Fernández, H. (2019). When does form reflect function? Acknowledging and supporting ecomorphological assumptions. Integr. Comp. Biol. *59*, 358–370.
29. Slater, G.J., and Friscia, A.R. (2019). Hierarchy in adaptive radiation: a case study using the Carnivora (Mammalia). Evolution *73*, 524–539.
30. Slater, G.J. (2022). Topographically distinct adaptive landscapes for teeth, skeletons, and size explain the adaptive radiation of Carnivora (Mammalia). Evolution *76*, 2049–2066.
31. Dávalos, L.M. (2007). Short-faced bats (Phyllostomidae: Stenodermatina): a Caribbean radiation of strict frugivores. J. Biogeogr. *34*, 364–375.
32. Rojas, D., Vale, A., Ferrero, V., and Navarro, L. (2011). When did plants become important to leaf-nosed bats? Diversification of feeding habits in the family Phyllostomidae. Mol. Ecol. *20*, 2217–2228.
33. Dumont, E.R., Dávalos, L.M., Goldberg, A., Santana, S.E., Rex, K., and Voigt, C.C. (2012). Morphological innovation, diversification and invasion of a new adaptive zone. Proc. Biol. Sci. *279*, 1797–1805.
34. Rossoni, D.M., Assis, A.P.A., Giannini, N.P., and Marroig, G. (2017). Intense natural selection preceded the invasion of new adaptive zones during the radiation of New World leaf-nosed bats. Sci. Rep. *7*, 11076.
35. Rossoni, D.M., Costa, B.M.A., Giannini, N.P., and Marroig, G. (2019). A multiple peak adaptive landscape based on feeding strategies and roosting ecology shaped the evolution of cranial covariance structure and morphological differentiation in phyllostomid bats. Evolution *73*, 961–981.
36. T.H. Fleming, L.M. Dávalos, and M.A. Mello, eds. (2020). Phyllostomid Bats: A Unique Mammalian Radiation (University of Chicago Press).
37. Freeman, P.W. (2000). Macroevolution in Microchiroptera: recoupling morphology and ecology with phylogeny. Evol. Ecol. Res. *2*, 317–333.
38. Baker, R.J., Bininda-Emonds, O.R.P., Mantilla-Meluk, H., Porter, C.A., and van den Bussche, R.A. (2012). Molecular time scale of diversification of feeding strategy and morphology in New World Leaf-Nosed Bats (Phyllostomidae): a phylogenetic perspective. In Evolutionary History of Bats: Fossils, Molecules and Morphology, G.F. Gunnell, ed. (Cambridge University Press), pp. 385–409.
39. Gunnell, G.F., Simmons, N.B., and Seiffert, E.R. (2014). New Myzopodidae (Chiroptera) from the Late Paleogene of Egypt: emended family diagnosis and biogeographic origins of Noctilionoidea. PLoS One *9*, e86712.
40. Hall, R.P., Mutumi, G.L., Hedrick, B.P., Yohe, L.R., Sadier, A., Davies, K.T.J., Rossiter, S.J., Sears, K.E., Dávalos, L.M., and Dumont, E.R. (2021). Find the food first: an omnivorous sensory morphotype predates biomechanical specialization for plant based diets in phyllostomid bats. Evolution *75*, 2791–2801.
41. Monteiro, L.R., and Nogueira, M.R. (2010). Adaptive radiations, ecological specialization, and the evolutionary integration of complex morphological structures. Evolution *64*, 724–744.
42. Monteiro, L.R., and Nogueira, M.R. (2011). Evolutionary patterns and processes in the radiation of phyllostomid bats. BMC Evol. Biol. *11*, 137.
43. Santana, S.E., Dumont, E.R., and Davis, J.L. (2010). Mechanics of bite force production and its relationship to diet in bats. Funct. Ecol. *24*, 776–784.
44. Santana, S.E., Strait, S., and Dumont, E.R. (2011). The better to eat you with: functional correlates of tooth structure in bats. Funct. Ecol. *25*, 839–847.
45. Santana, S.E., Grosse, I.R., and Dumont, E.R. (2012). Dietary hardness, loading behavior, and the evolution of skull form in bats. Evolution *66*, 2587–2598.
46. Dumont, E.R., Samadevam, K., Grosse, I., Warsi, O.M., Baird, B., and Davalos, L.M. (2014). Selection for mechanical advantage underlies multiple cranial optima in new world leaf-nosed bats. Evolution *68*, 1436–1449.
47. Hedrick, B.P., and Dumont, E.R. (2018). Putting the leaf-nosed bats in context: a geometric morphometric analysis of three of the largest families of bats. J. Mammal. *99*, 1042–1054.
48. Sadier, A., Davies, K.T., Yohe, L.R., Yun, K., Donat, P., Hedrick, B.P., Dumont, E.R., Dávalos, L.M., Rossiter, S.J., and Sears, K.E. (2018). Multifactorial processes underlie parallel opsin loss in Neotropical bats. eLife *7*, e37412.
49. Hedrick, B.P., Mutumi, G.L., Munteanu, V.D., S., A., Davies, K.T., Rossiter, S.J., Sears, K.E., Dávalos, L.M., and Dumont, E. (2020). Morphological diversification under high integration in a hyper diverse mammal clade. J. Mamm. Evol. *27*, 563–575.

50. Shi, J.J., Westeen, E.P., and Rabosky, D.L. (2021). A test for rate-coupling of trophic and cranial evolutionary dynamics in New World bats. Evolution *75*, 861–875.

51. López-Aguirre, C., Hand, S.J., Simmons, N.B., and Silcox, M.T. (2022). Untangling the ecological signal in the dental morphology in the bat superfamily Noctilionoidea. J. Mamm. Evol. *29*, 531–545.

52. Villalobos-Chaves, D., and Santana, S.E. (2022). Craniodental traits predict feeding performance and dietary hardness in a community of Neotropical free-tailed bats (Chiroptera: Molossidae). Funct. Ecol. *36*, 1690–1699.

53. Curtis, A.A., Smith, T.D., Bhatnagar, K.P., Brown, A.M., and Simmons, N.B. (2020). Maxilloturbinal aids in nasophonation in horseshoe bats (Chiroptera: Rhinolophidae). Anat. Rec. (Hoboken) *303*, 110–128.

54. Jackson, D.A. (1993). Stopping rules in principal components analysis: a comparison of heuristical and statistical approaches. Ecology *74*, 2204–2214.

55. Boyer, D.M. (2008). Relief index of second mandibular molars is a correlate of diet among prosimian primates and other euarchontan mammals. J. Hum. Evol. *55*, 1118–1137.

56. Slater, G.J., Price, S.A., Santini, F., and Alfaro, M.E. (2010). Diversity versus disparity and the radiation of modern cetaceans. Proc. Biol. Sci. *277*, 3097–3104.

57. Slater, G.J. (2013). Phylogenetic evidence for a shift in the mode of mammalian body size evolution at the Cretaceous-Palaeogene boundary. Methods Ecol. Evol. *4*, 734–744.

58. Clavel, J., Escarguel, G., and Merceron, G. (2015). mvMORPH: an R package for fitting multivariate evolutionary models to morphometric data. Methods Ecol. Evol. *6*, 1311–1319.

59. Bastide, P., Ané, C., Robin, S., and Mariadassou, M. (2018). Inference of adaptive shifts for multivariate correlated traits. Syst. Biol. *67*, 662–680.

60. Uyeda, J.C., Caetano, D.S., and Pennell, M.W. (2015). Comparative analysis of principal components can be misleading. Syst. Biol. *64*, 677–689.

61. Freeman, P.W. (1998). Form, function, and evolution in skulls and teeth of bats. In Bat Biology and Conservation, T.H. Kunz, ed. (Smithsonian Institution Press), pp. 140–156.

62. Clavel, J., and Morlon, H. (2020). Reliable phylogenetic regressions for multivariate comparative data: illustration with the MANOVA and application to the effect of diet on mandible morphology in phyllostomid bats. Syst. Biol. *69*, 927–943.

63. Mahler, D.L., Ingram, T., Revell, L.J., and Losos, J.B. (2013). Exceptional convergence on the macroevolutionary landscape in island lizard radiations. Science *341*, 292–295.

64. Yohe, L.R., Velazco, P.M., Rojas, D., Gerstner, B.E., Simmons, N.B., and Dávalos, L.M. (2015). Bayesian hierarchical models suggest oldest known plant-visiting bat was omnivorous. Biol. Lett. *11*, 20150501.

65. Polly, P.D. (2020). Functional tradeoffs carry phenotypes across the valley of the shadow of death. Integr. Comp. Biol. *60*, 1268–1282.

66. Goswami, A., Smaers, J.B., Soligo, C., and Polly, P.D. (2014). The macroevolutionary consequences of phenotypic integration: from development to deep time. Philos. Trans. R. Soc. Lond. B Biol. Sci. *369*, 20130254.

67. Harjunmaa, E., Kallonen, A., Voutilainen, M., Hämäläinen, K., Mikkola, M.L., and Jernvall, J. (2012). On the difficulty of increasing dental complexity. Nature *483*, 324–327.

68. Couzens, A.M.C., Sears, K.E., and Rücklin, M. (2021). Developmental influence on evolutionary rates and the origin of placental mammal tooth complexity. Proc. Natl. Acad. Sci. USA *118*, e2019294118.

69. Sadier, A., Anthwal, N., Krause, A.L., Dessalles, R., Lake, M., Bentolila, L.A., Haase, R., Nieves, N.A., Santana, S.E., and Sears, K.E. (2023). Bat teeth illuminate the diversification of mammalian tooth classes. Nat. Commun. *14*, 4687.

70. Jones, M.F., Li, Q., Ni, X., and Beard, K.C. (2021). The earliest Asian bats (Mammalia: Chiroptera) address major gaps in bat evolution. Biol. Lett. *17*, 20210185.

71. Evans, A.R., and Sanson, G.D. (2003). The tooth of perfection: functional and spatial constraints on mammalian tooth shape. Biol. J. Linn. Soc. Lond. *78*, 173–191.

72. Polly, P.D., Le Comber, S.C., and Burland, T.M. (2005). On the occlusal fit of tribosphenic molars: are we underestimating species diversity in the Mesozoic? J. Mamm. Evol. *12*, 283–299.

73. Luo, Z.X., Yuan, C.X., Meng, Q.J., and Ji, Q. (2011). A Jurassic eutherian mammal and divergence of marsupials and placentals. Nature *476*, 442–445.

74. Fleming, T.H., and Heithaus, E.R. (1986). Seasonal foraging behavior of the frugivorous bat *Carollia perspicillata*. J. Mammal. *67*, 660–671.

75. Villalobos-Chaves, D., Melo, F.P.L., and Rodríguez-Herrera, B. (2020). Dispersal patterns of large-seeded plants and the foraging behaviour of a frugivorous bat. J. Trop. Ecol. *36*, 94–100.

76. Villalobos-Chaves, D., Padilla-Alvárez, S., and Rodríguez-Herrera, B. (2016). Seed predation by the wrinkle-faced bat *Centurio senex*: a new case of this unusual feeding strategy in Chiroptera. J. Mammal. *97*, 726–733.

77. Freeman, P.W. (1988). Frugivorous and animalivorous bats (Microchiroptera) – dental and cranial adaptations. Biol. J. Linn. Soc. Lond. *33*, 249–272.

78. Rojas, D., Ramos Pereira, M.J., Fonseca, C., and Dávalos, L.M. (2018). Eating down the food chain: generalism is not an evolutionary dead end for herbivores. Ecol. Lett. *21*, 402–410.

79. Todd Streelman, J.T., and Danley, P.D. (2003). The stages of vertebrate evolutionary radiation. Trends Ecol. Evol. *18*, 126–131.

80. Rolfe, S., Pieper, S., Porto, A., Diamond, K., Winchester, J., Shan, S., Kirveslahti, H., Boyer, D., Summers, A., and Maga, A.M. (2021). SlicerMorph: an open and extensible platform to retrieve, visualize and analyse 3D morphology. Methods Ecol. Evol. *12*, 1816–1825.

81. Polly, P.D. (2022). Geometric Morphometrics for Mathematica, version 12.4 (Department of Geological Sciences, Indiana University).

82. Revell, L.J. (2012). phytools: an R package for phylogenetic comparative biology (and other things). Methods Ecol. Evol. *3*, 217–223.

83. Pinheiro, J.C., and Bates, D.M.; R Core Team (2023). Nlme: linear and nonlinear mixed effects models. R package version 3.1-162.

84. Pennell, M.W., Eastman, J.M., Slater, G.J., Brown, J.W., Uyeda, J.C., FitzJohn, R.G., Alfaro, M.E., and Harmon, L.J. (2014). geiger v2.0: an expanded suite of methods for fitting macroevolutionary models to phylogenetic trees. Bioinformatics *30*, 2216–2218.

85. Shi, J.J., Westeen, E.P., and Rabosky, D.L. (2018). Digitizing extant bat diversity: an open-access repository of 3D μCT-scanned skulls for research and education. PLoS One *13*, e0203022.

86. Nowak, R.M. (1999). Walker's Mammals of the World (John Hopkins University Press).

87. Wilman, H., Belmaker, J., Simpson, J., de la Rosa, C., Rivadeneira, M.M., and Jetz, W. (2014). EltonTraits 1.0: species-level foraging attributes of the world's birds and mammals. Ecology *95*, 2027.

88. Cooper, N., Thomas, G.H., Venditti, C., Meade, A., and Freckleton, R.P. (2016). A cautionary note on the use of Ornstein Uhlenbeck models in macroevolutionary studies. Biol. J. Linn. Soc. Lond. *118*, 64–77.

89. Pineda-Munoz, S., and Alroy, J. (2014). Dietary characterization of terrestrial mammals. Proc. Biol. Sci. *281*, 20141173.

90. Pellón, J.J., Medina-Espinoza, E.F., Lim, B.K., Cornejo, F., and Medellín, R.A. (2023). Eat what you can, when you can: relatively high arthropod consumption by frugivorous bats in Amazonian Peru. Mamm. Biol. *103*, 137–144.

91. Reuter, D.M., Hopkins, S.S.B., and Price, S.A. (2023). What is a mammalian omnivore? Insights into terrestrial mammalian diet diversity, body mass and evolution. Proc. Biol. Sci. *290*, 20221062.

92. Santana, S.E., Grossnickle, D.M., Sadier, A., Patterson, E., and Sears, K.E. (2022). Bat dentitions: a model system for studies at the interface

of development, biomechanics, and evolution. Integr. Comp. Biol. *62*, 762–773.

93. Wilson, G.P. (2013). Mammals across the K/Pg boundary in northeastern Montana, USA: dental morphology and body-size patterns reveal extinction selectivity and immigrant-fueled ecospace filling. Paleobiology *39*, 429–469.
94. Grossnickle, D.M., and Newham, E. (2016). Therian mammals experience an ecomorphological radiation during the Late Cretaceous and selective extinction at the K–Pg boundary. Proc. R. Soc. B. *283*, 20160256.
95. Selig, K.R., Sargis, E.J., and Silcox, M.T. (2019). Three-dimensional geometric morphometric analysis of treeshrew (Scandentia) lower molars: insight into dental variation and systematics. Anat. Rec. *302*, 1154–1168.
96. Bookstein, F.L. (1997). Morphometric Tools for Landmark Data (Cambridge University Press).
97. R Development Core Team (2020). R: A Language and Environment for Statistical Computing, version 4.1.3 (R Foundation for Statistical Computing).
98. Upham, N.S., Esselstyn, J.A., and Jetz, W. (2019). Inferring the mammal tree: species-level sets of phylogenies for questions in ecology, evolution, and conservation. PLoS Biol. *17*, e3000494.
99. Velazco, P.M. (2005). Morphological phylogeny of the bat genus *Platyrrhinus* Saussure, 1860 (Chiroptera: Phyllostomidae) with the description of four new species. Fieldiana Zool. *2005*, 1–53.
100. Wetterer, A.L., Rockman, M.V., and Simmons, N.B. (2000). Phylogeny of phyllostomid bats (Mammalia: Chiroptera): data from diverse morphological systems, sex chromosomes, and restriction sites. Bull. Am. Mus. Nat. Hist. *248*, 1–200.
101. Hansen, T.F. (1997). Stabilizing selection and the comparative analysis of adaptation. Evolution *51*, 1341–1351.
102. Butler, M.A., and King, A.A. (2004). Phylogenetic comparative analysis: a modeling approach for adaptive evolution. Am. Nat. *164*, 683–695.
103. Freckleton, R.P., and Harvey, P.H. (2006). Detecting non-Brownian trait evolution in adaptive radiations. PLoS Biol. *4*, e373.
104. Bollback, J.P. (2006). SIMMAP: stochastic character mapping of discrete traits on phylogenies. BMC Bioinformatics *7*, 88.
105. Bartoszek, K., Pienaar, J., Mostad, P., Andersson, S., and Hansen, T.F. (2012). A phylogenetic comparative method for studying multivariate adaptation. J. Theor. Biol. *314*, 204–215.

Please cite this article in press as: Grossnickle et al., The hierarchical radiation of phyllostomid bats as revealed by adaptive molar morphology, Current Biology (2024), https://doi.org/10.1016/j.cub.2024.02.027

STAR★METHODS

KEY RESOURCES TABLE

REAGENT or RESOURCE	SOURCE	IDENTIFIER
Biological samples		
Noctilionoid bat skeletons – specimen information is in Data S1	AMNH, UWBM, UMMZ, MorphoSource	https://www.morphosource.org/
Deposited data		
Molar landmark coordinates and basicranium widths are provided in Data S1	N/A	N/A
Software and algorithms		
3DSlicer	N/A	https://www.slicer.org/
SlicerMorph	Rohlf et al.[80]	https://slicermorph.github.io/
Geometric morphometrics for Mathematica	Polly[81]	https://github.com/pdpolly/Morphometrics-for-Mathematica
mvMORPH R package	Clavel et al.[58]	https://cran.r-project.org/web/packages/mvMORPH/index.html
phytools R package	Revell[82]	https://cran.r-project.org/web/packages/phytools/index.html
nlme R package	Pinheiro et al.[83]	https://cran.r-project.org/web/packages/nlme/index.html
geiger R package	Pennell et al.[84]	https://cran.r-project.org/web/packages/geiger/index.html

RESOURCE AVAILABILITY

Lead contact

Further information and requests for resources and data should be directed to and will be fulfilled by the lead contact, David M. Grossnickle (david.grossnickle@oit.edu).

Materials availability

This study did not generate new unique reagents.

Data and code availability

Molar shape data (3D landmark coordinates) and basicranium widths are provided in Data S1B, and bat micro-CT scans will be uploaded to the MorphoSource repository (https://www.morphosource.org/) upon publication. This paper did not produce new *R* or *Mathematica* code functions, but our scripts that implement published functions are available from the lead contact upon request.

EXPERIMENTAL MODEL AND STUDY PARTICIPANT DETAILS

Our sample consists of noctilionoid bat skulls. Specimens are primarily from the American Museum of Natural History (AMNH), Burke Museum of Natural History & Culture (UWBM), and the University of Michigan Museum of Zoology (UMMZ). Data S1B provides information on the specimens.

METHOD DETAILS

We collected micro-computed tomography (μCT) scans of 405 noctilionoid bat skulls. We excluded specimens with worn or fractured first lower molars, resulting in a final sample of 315 specimens, representing 125 species and 56 genera (Data S1B). Scanning was performed at the University of Washington using Bruker's Skyscan 1172 and 1173 μCT scanners. Further, our sample includes scans obtained from the MorphoSource online repository (https://www.morphosource.org/); many of these scans are available due to a recent effort to digitize bat diversity.[85] The μCT image stacks were imported into 3DSlicer using SlicerMorph ImageStacks[80] and then converted to mesh models using 3DSlicer.

Dietary classifications of species are based on multiple sources (Data S1A; supplemental information), including López-Aguirre et al.,[51] Rojas et al.,[78] and two compendiums.[86,87] We used two different classifications schemes: a three-diet scheme and a four-diet scheme. The four-diet scheme includes faunivory (broadly including insectivory, carnivory, and piscivory), frugivory, nectarivory, and omnivory. The three-diet scheme excludes omnivory as a category, and omnivorous species are classified into the other three-diet groups based on their preferred food items (Data S1A). We excluded sanguivores because their first lower molar is too derived for collection of landmarks for geometric morphometrics (Figure S3). Further, extant sanguivores are represented by only

Please cite this article in press as: Grossnickle et al., The hierarchical radiation of phyllostomid bats as revealed by adaptive molar morphology, Current Biology (2024), https://doi.org/10.1016/j.cub.2024.02.027

three species within a single clade (Desmodontinae), meaning that the sample size is too small to be appropriate for defining sanguivory as a separate selective regime in evolutionary model-fitting analyses.[88] See Data S1A for more information.

Classification of omnivores is especially challenging and subjective.[15,89–91] We chose to only classify species as omnivores if the animal and plant components of their diets are approximately equal. This is a more restrictive definition of omnivory than that used in Rojas et al.[78] For the three-diet scheme, which excludes omnivory as a category, the omnivorous species are classified into the other three diet groups based on their preferred food items and/or their ancestral diets (Data S1A).

We collected morphometric data (see below) on the first lower molar (m1) because it is present in all taxa and is easily identifiable, and it has especially strong functional importance in bats.[51,92] For body size analyses, we used natural log-transformed basicranium widths as proxies for body size[53]; other cranial size metrics such as skull length are heavily influenced by diet (e.g., nectarivores have disproportionately long rostra). Because complete skulls were not available for all scanned specimens, our sample for basicranium width analyses (n = 122 species) excluded *Enchisthenes hartii*, *Lonchophylla handleyi*, and *Vampyressa melissa*.

QUANTIFICATION AND STATISTICAL ANALYSIS

Geometric morphometrics and analyses of PCs

We quantified m1 shape using geometric morphometrics, which included collecting 3D landmark coordinates (Data S1C). Previous studies have demonstrated that geometric morphometric analyses of molar shape can differentiate diet groups.[93–95] Five landmarks (1–4, 7) are tips of molar cusps, one landmark (6) is at a specific position on a molar crest (6), and the remaining landmarks (5, 8–10) are Type III landmarks[96] that help to capture general molar shape. The 10 landmarks are shown in Figure 1A and are summarized here: 1) paraconid, 2) protoconid, 3) metaconid, 4) entoconid, 5) deepest point of the talonid basin, 6) mesial-most point of the cristid obliqua at the junction with the trigonid, 7) hypoconid, 8) labial-most point (in occlusal view) at the base of the talonid region/hypconid, 9) labial-most point (in occlusal view) at the base of the trigonid region/protoconid, 10) lingual-most point (in occlusal view) at the base of the metaconid, approximately at the midpoint of the length of the molar. For landmark 5, in taxa with especially flat 'basins' (e.g., many frugivores), we used the center of the talonid basin region, approximately equidistant from surrounding cusps. For landmarks 8–10, we placed the landmark on the cingulum if present.

We accounted for differences in molar size and orientation via a generalized Procrustes superimposition. For species represented by more than one specimen, we calculated species means using Procrustes values, and we used these means in subsequent analyses. We ordinated and reduced the dimensionality of the Procrustes aligned coordinates using a principal component analysis (PCA). We used functions in the *Geometric Morphometrics for Mathematica* package[81] for these analyses. We produced a PC1–2 phylomorphospace plot (Figure 1C) using the *phylomorphospace* function in the *phytools* package[82] for *R*.[97] The phylogeny (Figure 1B) used for the phylomorphospace and subsequent comparative analyses is a maximum clade credibility tree of 500 trees from the posterior distribution of the 'completed trees' analysis of Upham et al.[98] We used a 'broken-stick' model[54] to determine which PCs account for more variance than expected by chance (Figure S4).

In many frugivores, the homology of cusps is uncertain due to the evolutionary loss or gain of cusps.[61,99,100] In some cases, we made subjective decisions for the locations of the paraconid and metaconid landmarks, and when there was a lack of candidate cusps (i.e., the paraconid and/or metaconid appeared to have been evolutionarily lost), we placed landmark points in the presumed homologous region. To help account for this uncertainty in landmark locations among frugivores, we repeated analyses using two landmarking schemes with alternative positions for the paraconid and metaconid landmarks (Landmarks 1 and 3) for some frugivores (n = 20 species; Figure S1; Data S1B). We refer to these as the 'outer' and 'inner' landmarking schemes, with the 'outer' scheme being used for our primary results. See Figure S1 and Data S1B for more information.

Analyses using the alternative landmarking schemes serve as a sensitivity test for the influence of uncertain landmark positions on our results. The results of analyses using the 'inner' landmarking scheme (Tables S4–S6) are very similar to those of the 'outer' landmarking scheme (Tables 2, 3, and S3), and thus we do not believe that the uncertain positions of some landmarks have an influence on our broad conclusions. However, frugivores exhibit a stronger early burst signal when using the 'inner' landmarking scheme (Table S6).

To determine which PCs are most closely linked to diet, we performed phylogenetic analyses of variance (pANOVAs) by regressing the scores of individual PCs against discrete diet categories (for both the three-diet scheme and four-diet scheme) using phylogenetic generalized least squares (PGLSs) via the *gls* function in the *nlme* library,[83] and then applying an ANOVA test. We incorporated phylogenetic signal into the regressions using maximum likelihood (i.e., the 'lambda' model setting). Further, we performed pMANOVAs on all molar shape data (and repeated using only PC1–2) to test for differences in molar shape among diet groups. These were performed using the *mvgls* and *manova.gls* functions of *mvMORPH*[58,62] with 9999 permutations (Table S1). We used the 'lambda' model that transforms phylogenetic branch lengths based on the measured phylogenetic signal. We repeated the pMANOVAs using an EB model for PC1–2 and an OU model for complete molar data (i.e., all Procrustes residuals) because these models were best-fitting to the respective datasets (Figure 3; Table S3). The choice of method does not appear to influence the results, which are strongly significant using any methodology (Table S1).

Evolutionary model-fitting analyses

We fit a suite of evolutionary models to morphological datasets using functions in the *mvMORPH R* library.[58] These include three classes of evolutionary models: single-selective-regime (or uniform) models, 'shift' models, and multiple-selective-regime models.

Please cite this article in press as: Grossnickle et al., The hierarchical radiation of phyllostomid bats as revealed by adaptive molar morphology, Current Biology (2024), https://doi.org/10.1016/j.cub.2024.02.027

The single-regime models are BM1 ('random walk'), OU1 (random walk with a selection parameter[101,102]), and EB (random walk with a rate decay parameter[10,103]). The shift models[57,58] allow for a shift in mode of evolution (e.g., OUBM models a shift from OU to BM) and/or shift in rate (e.g., BMBM only includes a shift in rate) at Phyllostomidae*. We chose to test for a shift at Phyllostomidae* because most phyllostomid dietary diversity appears to rapidly evolve after that node (Figure 1C). For multiple-regime models, the selective regimes correspond to diet group classifications. Three-regime models (BM1m3, BMM3, OUM3) use the three-diet classification scheme, and four-regime models (BM1m4, BMM4, OUM4) use the four-diet classification scheme, which includes omnivory as a category. BM1m models allow the phylogenetic means to vary among regimes but keep the evolutionary rate (σ^2) constant, whereas BMM models allow differences in rates between regimes. The reported evolutionary rates (Table 2) are the σ^2 (rate-step) parameter from the BMM3 model, which was the best-fitting model to the full sample. Multiple-regime OU models (OUM) allow trait optima to vary among regimes, but σ^2 and α remain constant. We drop the root state influence (i.e., root = "stationary") because we are using an ultrametric tree without fossil evidence for the root state.[58] Model support was determined using small-sample-size-corrected Akaike Information Criterion (AICc) values.

We performed two sets of model-fitting analyses: 'full-sample analyses' and 'subgroup analyses.' We repeated each set of analyses using three morphological datasets: molar correlates of diet (PC1–2, 62% of variance), overall molar shape (PC1–6, 85% of variance), and basicranium widths. For molar analyses, the evolutionary models are multivariate. We limited the 'overall molar shape' analyses to the first six PCs due to computational constraints. The two sets of analyses are summarized here:

(i) Full-sample analyses. Using all species in our sample (n = 125), we fitted single-regime, shift, and multiple-regime evolutionary models to morphological data. The inclusion of multiple-regime models allowed us to test for the presence of multiple diet-affiliated adaptive zones, and to test whether omnivores occupy a distinct adaptive zone. For multiple-regime models, the ancestral diet histories were reconstructed on the phylogeny using stochastic character maps (i.e., SIMMAPs[104]), produced using the *make.simmap* function of the *phytools* library[82] and an equal rates model. The reported results are means from using 25 SIMMAP trees.

(ii) Subgroup analyses. Using separate analyses for different subclades and specific diet groups (see results and Figure 3), we fitted single-regime evolutionary models to morphological data. Prior to analyses, we pruned the phylogeny to the focal lineages for each analysis. Because of smaller sample sizes and the focus on within-adaptive zone/regime patterns, we only fitted single-regime models in these analyses.

To independently test for selective regime shifts that are not based on *a priori* regime (diet) assignments, we used the *phyloEM* function and *scalar OU* model in the *PhylogeneticEM* R package.[59] This function automatically detects regime shifts (in a multiple-regime OU context) while accounting for correlations among traits. We tested 100 α values for three parallel computations and repeated analyses using PC1–2 and PC1–6. The PC1–2 analysis identified three-regime shifts (Figure S5), which occurred on the branches leading to three major phyllostomid subclades (Glossophaginae, Lonchophyllinae, Stenodermatinae). The three shifts were within Phyllostomidae (Figure S5) and mostly correspond to dietary shifts: two shifts at the base of nectarivore clades (Glossophaginae and Lonchophyllinae) and the third shift is at the base of the major frugivore clade (Stenodermatinae). This is largely consistent with results for the 'full-sample' model-fitting analyses with *a priori* regime assignments (Table 3). The *phyloEM* analysis using PC1–6 indicated 13 regime shifts with >400 equivalent solutions with shift locations at various positions in the phylogeny. We interpret the diversity of solutions for PC1–6 to be less indicative of a diet-affiliated early burst pattern because the shift positions vary within the phylogeny and often do not correspond to major dietary changes.

Morphological disparity

We calculated morphological disparity by summing variances of the data (either PCs 1 and 2 for analyses of diet correlates or all Procrustes residuals for analyses of overall molar shape) for each focal group. Further, we measured the stationary variances (expected variance when an OU process has reached a stationary state; $\sigma^2/2\alpha$) of PC1 and PC2 scores for each of the diet groups (Table S2), using the fitted OU1 evolutionary models and *stationary* function from the *mvMORPH* R package.[58,105] We used the *disparity-through-time* (*dtt*) function from the *geiger R* library[84] to plot the average subclade disparity through time (Figure 2) and calculate the MDI statistic,[8,56] with 1000 BM-evolved simulations for null disparity patterns. MDI is the area between the DTT for the data and the median of the simulations, with *p-value*s based on the probability that the MDI is significantly more negative than expected under a BM model.[8,56] As supplemental tests of early bursts, we performed node height tests[26,103] by fitting linear models to independent contrasts versus node heights via the *nh.test* function in the *geiger R* library.[84] A significant, negative relationship reflects greater contrasts earlier in the focal clade's history, providing evidence for an early burst.